JOURNAL OF MATERIALS SCIENCE **36** (2001) 3503 – 3510

Chemical vapor deposition of carbon from methane at various pressures, partial pressures and substrate surface area/reactor volume ratios

W.G. ZHANG, K. J. HÜTTINGER*
Institut für Chemische Technik, Universität Karlsruhe, Kaiserstr. 12, D - 76128 Karlsruhe, Germany
E-mail: wgzhang@ict.uni-karlsruhe.de; huettinger@ict.uni-karlsruhe.de

Carbon deposition from methane was studied as a function of substrate length at a temperature of 1100 °C, total pressures ranging from 90 to 10 kPa at a constant methane partial pressure of 10 kPa, methane pressures ranging from 5 to 20 kPa, and residence times of 0.55 s and 1.1 s using substrates with surface area/volume ratios of 0.78, 1.65 and 3.55 mm^{-1}. Various total pressures at constant methane pressure have significant influences on the deposition profile of carbon, but they are mainly caused by different boundary conditions. The methane pressure reference suggests saturation adsorption (Langmuir - Hinshelwood kinetics) upto a pressures of about 15 kPa. Increasing surface area/volume ratios leads to decreasing surface related deposition rates, because the deposition chemistry is changed.

1. Introduction

Isothermal, isobaric chemical vapor deposition (CVD) of carbon from light hydrocarbons exhibits a remarkable history, because it is a key process for the production of several advanced products [1]. Performed in the diffusion mode, usually described as chemical vapor infiltration (CVI), it represents the most important process for the production of carbon fiber reinforced carbon [2].

The literature on these processes and the advantages of methane for CVI have recently been summarized [3]. Based on experimental studies it was shown that CVD of carbon from light hydrocarbons and especially from methane is a homogeneous-heterogeneous reaction [4–7]. Homogeneous reactions in the gas phase lead to hydrocarbons with increasing size or molecular mass (aromatic and polyaromatic hydrocarbons). Heterogeneous reactions are controlled by active sites at the carbon surface. Formation of hydrocarbon species with increasing molecular mass in the gas phase implies increasing deposition rates [5, 6]; this can easily be understood assuming that one active site is needed for chemisorption of any reactive hydrocarbon species from the gas phase. Hydrogen, added to the feed gas or formed in gas phase reactions, can block free active sites by formation of extremely stable carbon-hydrogen surface complexes, $C_\infty(H)$, and thus inhibit the deposition reactions [8]. This hydrogen inhibition is very selective with respect to the carbon/hydrogen ratio and the molecular structure of a carbon forming species. In the case of light linear species inhibition increases with decreasing C/H ratio, in the case of aromatic or polyaromatic species it is dramatic or even complete, although these species exhibit a higher C/H ratio than ethine.

In any kind of deposition process, the interaction of homogeneous and heterogeneous reactions is determined by the substrate surface area/reactor volume ratio, $[A_S/V_R]$ [7, 9, 10]. Changing this parameter causes a change of deposition chemistry and thus of deposition kinetics. At a low ratio (low surface area), gas phase reactions are favored and aromatic and polyaromatic species are rapidly formed, i.e. carbon is mainly deposited from these species. At a high or very high ratio reactive species formed in initial gas phase reactions may immediately chemisorb at the surface and form carbon; thus formation of aromatic and polyaromatic species in the gas phase is limited. As the rates of carbon deposition from large species are higher than those from small species, surface related rates depend on $[A_S/V_R]$ ratio and may never be constant.

The significance of this ratio for CVI is obvious because the internal surface area/pore volume ratio continuously increases with progressive infiltration. For this reason, this ratio was introduced as the third parameter of CVD, besides temperature, pressure or partial pressure [7, 11].

The mentioned results were obtained from CVD experiments at pressures of 100 or 90 kPa, using argon as a diluent gas. For a CVD performed in the diffusion mode (CVI) low pressures are required. Thus, carbon deposition was investigated at constant methane partial

*Author to whom all correspondence should be addressed.

pressures and decreasing total pressure (by decreasing the argon partial pressure) as well as at various methane pressures (without argon). The substrate surface area/reactor volume ratio was varied from 0.78 to 1.65 and 3.55 mm^{-1}.

In the earlier investigations the residence time was varied at constant substrate length or surface area using various gas flow rates. As deposition reactors exhibit the characteristics of a tubular reactor with changing composition of the gas phase along the reactor axis [12] the deposition rates were determined as a function of the reactor/substrate length.

A variation of total pressure at a given residence time implies different volume flows; additionally, it changes the diffusion rates in radial as well as axial direction. The consequences on the flow profiles as well as the gas temperatures were analyzed by corresponding simulation studies using FLUENT 5.2 [13].

2. Experimental

The deposition reactor was similar to that used in earlier studies [4, 9, 10], except that the substrate length was increased from 20 to about 37 mm. A cross section is shown in Fig. 1. The deposition space is formed by an alumina ceramic tube, 22 mm in diameter and 40 mm in length. Channel structures, made of cordierite, with 25, 100 and 400 channels per $inch^2$ were fitted in the alumina ceramic tube in order to vary $[A_S/V_R]$ ratio. Each channel structure was composed of 8 slices, each about 4.62 mm in length. Some geometric properties of the channel structures are compiled in Table I. The volumes for the channel structures are nearly equal, i.e an increasing $[A_S/V_R]$ ratio results from an increasing A_S. The pores of the cordierite were filled by precoating with carbon until a steady-state deposition rate was achieved. Steady-state deposition rates were determined from the mass gain of the substrate slices after two or three subsequent deposition experiments of about 8 hours.

Methane used as a carbon source gas had a purity of 99.5% (major impurity ethene up to 0.3%); that of argon (diluent gas) was 99.998%. The composition of the gas phase as a function of residence time was analyzed after passing a cold trap using a gas chromatography equipped with a thermal conductivity detector.

TABLE I Some geometric properties of the channel structures

Channel density, cpsi[1)]	25	100	400
Wall thickness, mm	0.889	0.381	0.178
V_R, 10^3 mm^3 [2)]	10.064	10.342	10.415
A_S, 10^3 mm^2 [2), 3)]	7.844	17.08	37
$[A_S/V_R]$, mm^{-1}	0.779	1.65	3.55
Open porosity,vol%	68.1	72.3	74.0

1) channels per square inch;
2) Corresponding to an average length of 37 mm (the real lengths ranged from 34 - 39 mm);
3) A_S considers the surface area of the channel structure, because the mass gain of the channel structure has been determined after each deposition, only.

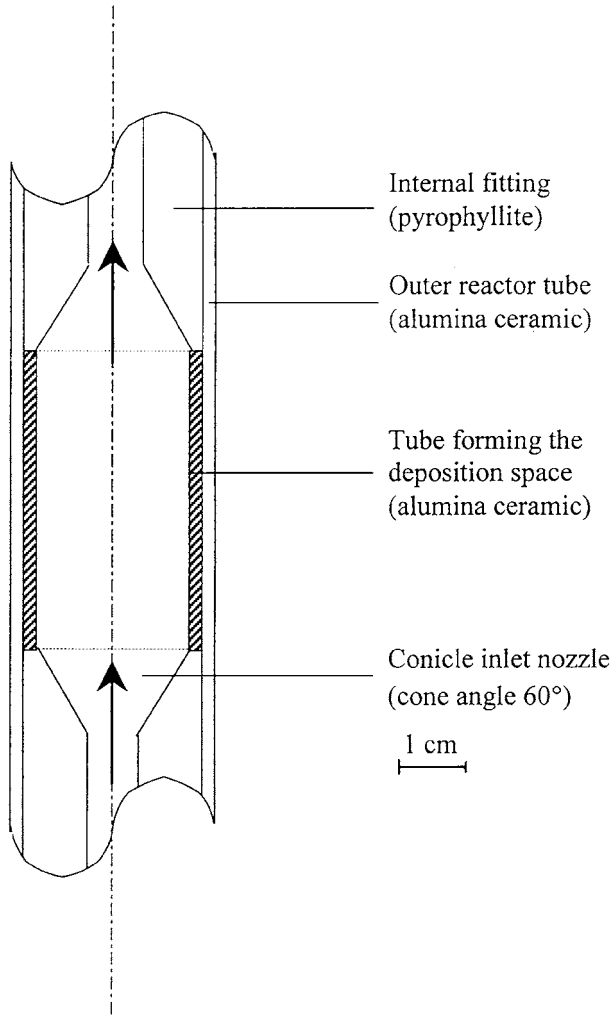

Figure 1 Scheme of the deposition reactor.

3. Results

3.1. Various total pressures at constant methane partial pressure

All deposition experiments were performed at a temperature of 1100 °C, which is relevant for CVI of carbon from methane. Results obtained at a methane partial pressure of 10 kPa and total pressures of 90, 50, 30 and 10 kPa are presented in Fig. 2 ($[A_S/V_R] = 0.78\ mm^{-1}$) and Fig. 3 ($[A_S/V_R] = 1.65\ mm^{-1}$). These figures show surface related deposition rates of carbon as a function of reactor/substrate length at two different volume flows, corresponding to residence times (calculated from the length of the substrates of about 37 mm) of 0.55 s (Fig. a) and 1.1 s (Fig. b). The rates generally increase with increasing reactor length l or increasing relative residence time τ_R (see Equation 1).

$$\tau_R = \frac{1}{\bar{u}} \tag{1}$$

$\bar{u}$ = mean gas flow rate.

The effects of total pressure, residence time and $[A_S/V_R]$ ratio are significant. Increasing pressure leads to decreasing initial deposition rates. The rate increase as a function of reactor length is linear at 10 kPa (pure methane) and exponential at all higher pressures of 30, 50 and 90 kPa. The initial rates as well as the slopes

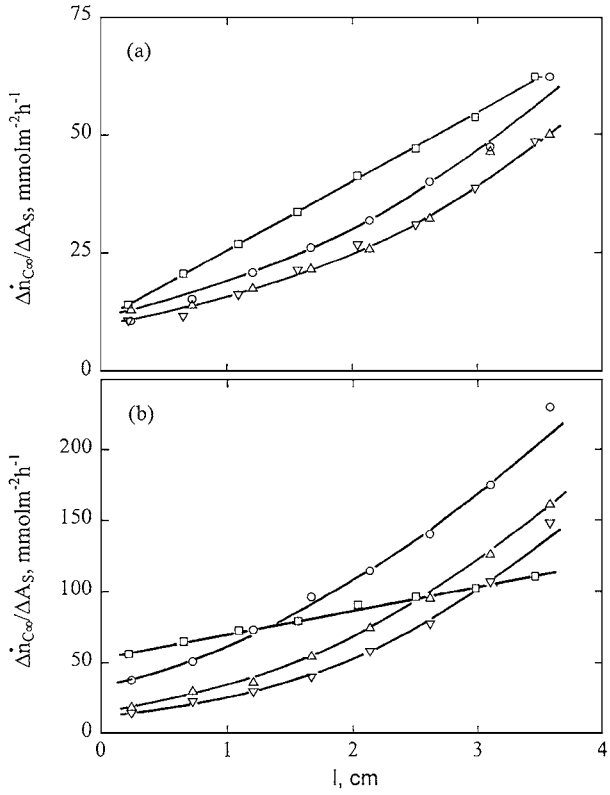

Figure 2 Steady-state surface related deposition rates as a function of substrate length at a temperature of 1100 °C, a constant methane partial pressure of 10 kPa at various total pressures and a $[A_S/V_R]$ ratio of 0.78 mm^{-1}; the residence times are (a) 0.55 s and (b) 1.1 s. (□) 10 kPa, (○) 30 kPa, (△) 50 kPa and (▽) 90 kPa.

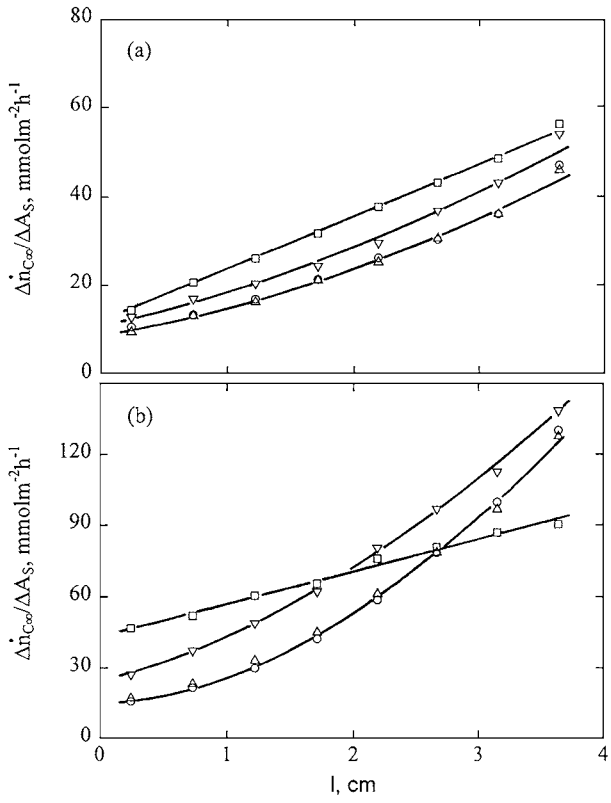

Figure 3 Steady-state surface related deposition rates as a function of substrate length at a temperature of 1100 °C, a constant methane partial pressure of 10 kPa at various total pressures and a $[A_S/V_R]$ ratio of 1.65 mm^{-1}; the residence times are (a) 0.55 s and (b) 1.1 s. Symbols see Fig. 2.

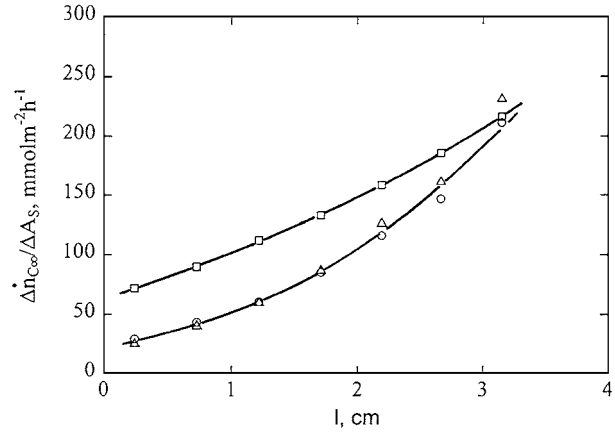

Figure 4 Steady-state surface related deposition rates as a function of substrate length at a temperature of 1100 °C, a constant methane partial pressure of 20 kPa at various total pressures and a $[A_S/V_R]$ ratio of 1.65 mm^{-1}; the residence time is 1.1 s. (□) 20 kPa, (○) 50 kPa and (△) 90 kPa.

of the rate increase are strongly influenced by the residence time. The slopes at 10 kPa are lowered, those at the higher pressures are increased by changing the residence time from 0.55 s to 1.1 s. The influence of $[A_S/V_R]$ ratio is small at 0.55 s, but significant at 1.1 s residence time; the surface related rates at a ratio of 0.78 mm^{-1} are clearly lower than those at a ratio of 1.65 mm^{-1}. The latter result is similar to those obtained in earlier studies [6] by variation of residence time at constant reactor or substrate length.

Results on the influence of total pressure at a methane partial pressure of 20 kPa are presented in Fig. 4. A comparison with the results at 10 kPa methane partial pressure (Fig. 3b) shows that the deposition rates at 20 kPa are higher and exhibit a much stronger increase along the substrate. At 20 kPa pressure (pure methane) an exponential rate increase can be observed, additionally.

Results obtained with all three substrates at two different total pressures of 90 and 10 kPa are presented in Figs. 5 and 6. Surface related deposition rates at 90 kPa and a residence time of 1.1s (Fig. 5) are nearly

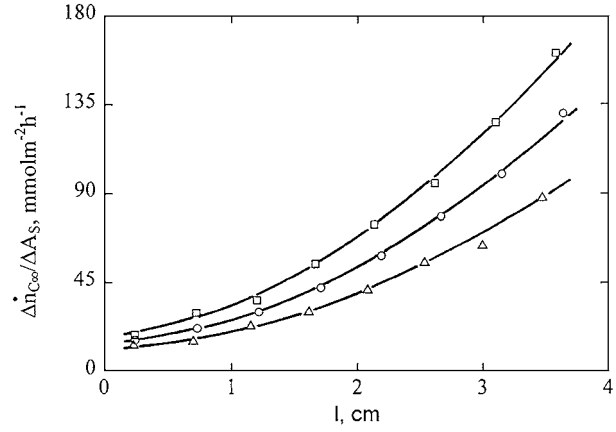

Figure 5 Steady-state surface related deposition rates as a function of substrate length at a temperature of 1100 °C, a constant methane partial pressure of 10 kPa at a total pressure of 90 kPa; the residence time is 1.1 s. (□) $[A_S/V_R] = 0.78$ mm^{-1}, (○) $[A_S/V_R] = 1.65$ mm^{-1}, and (△) $[A_S/V_R] = 3.55$ mm^{-1}.

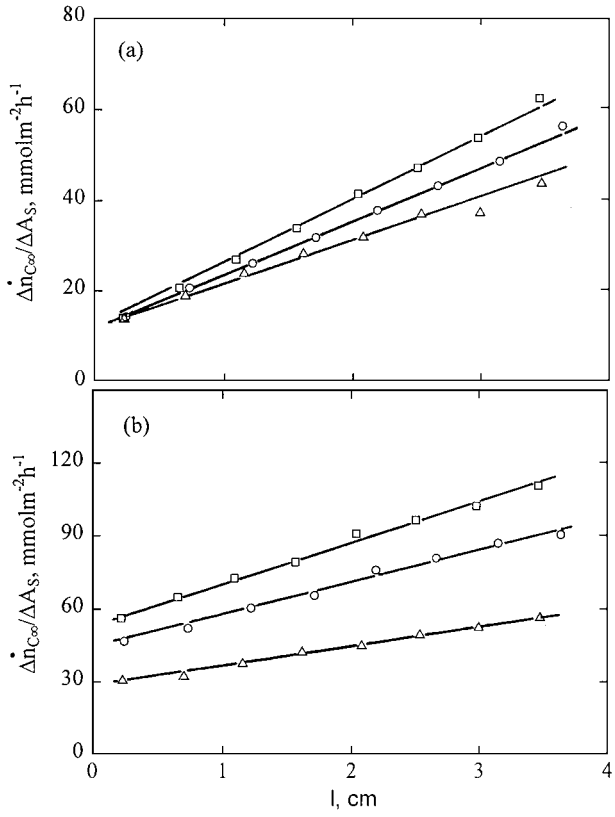

Figure 6 Steady-state surface related deposition rates as a function of substrate length at a temperature of 1100 °C, a methane partial pressure of 10 kPa; the residence times are (a) 0.55 s and (b) 1.1 s. Symbols see Fig. 5.

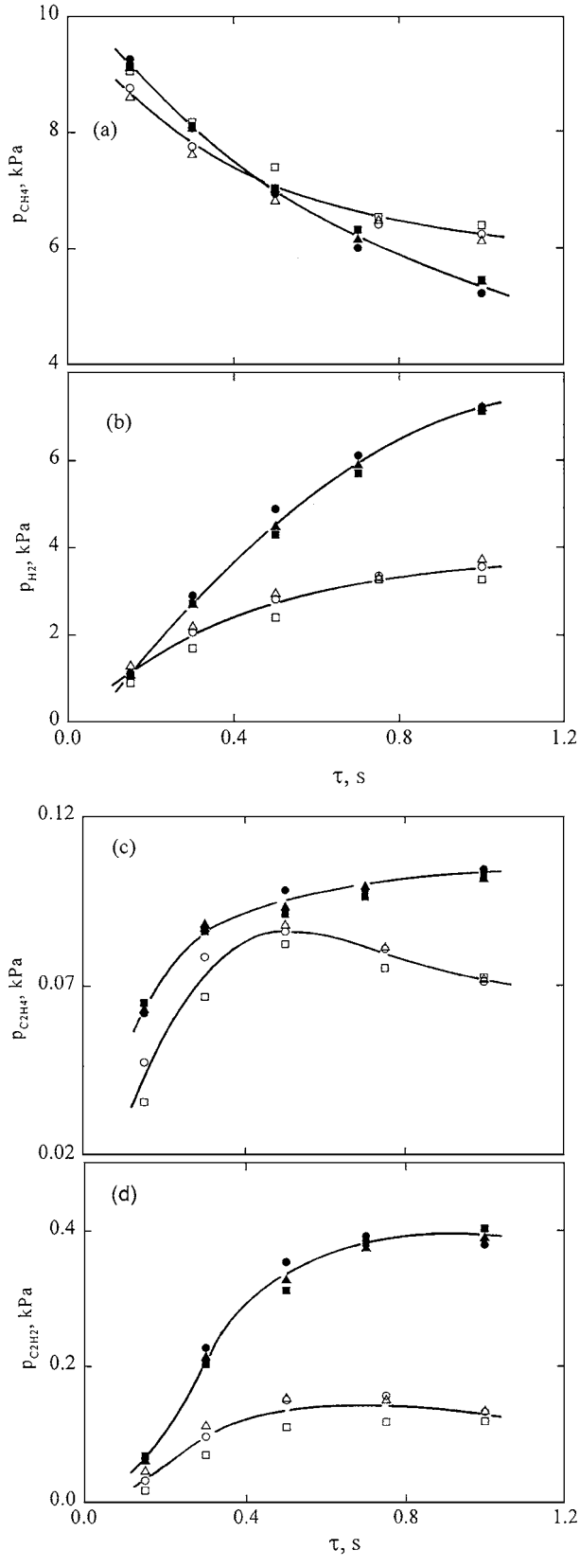

Figure 7 Results of the gas phase analysis at a temperature of 1100 °C, pressures of 100 kPa (90 kPa argon and 10 kPa methane: filled symbols) and 10 kPa (methane: open symbols) and three $[A_S/V_R]$ ratios (symbols see Fig. 5) showing partial pressures as a function of residence time (determined for unconverted methane at 1100 °C); (a) methane, (b) hydrogen, (c) ethene and (d) ethine.

independent of $[A_S/V_R]$ ratio at the beginning of the substrate. Differences develop as the gas flows along the substrate leading to rates at the end of the substrates which differ by a factor of two if $[A_S/V_R]$ ratio is changed by a factor of 4.5.

A similar result is obtained at 10 kPa (pure methane) and 0.55 s, at least as far as the initial rates are concerned (Fig. 6a). The influence of $[A_S/V_R]$ ratio on the deposition rates as a function of substrate length at the short residence time of 0.55 s is obvious, but less pronounced if compared to that at 90 kPa and 1.1 s (Fig. 5).

A significant effect can also be seen at 10 kPa and a residence time of 1.1s (Fig. 6b). The surface related deposition rates at $[A_S/V_R]$ ratios of 0.78 and 3.55 mm^{-1} differ by a factor of two not only at the end, but also at the beginning of the substrate.

Under ideal conditions of deposition, the deposition rates at the end of the substrate at 0.55 s (Fig. 6a) should be identical to those at the middle of the substrate at 1.1 s (Fig. 6b). In fact, the latter rates are slightly higher. This discrepancy results from the boundary conditions of a flow reactor [12]. Decreasing the volume flow leads to a longer residence time of the gas in the pre-heating zone of the reactor. This may cause not only a more complete pre-heating, but also pyrolysis reactions of methane by formation of larger hydrocarbon species which form carbon at a higher rate.

Gas analyses were performed as a function of residence time at pressures of 10 kPa (pure methane) and 100 kPa (10 kPa methane partial pressure) with all three substrates. The results are presented in Fig. 7a–d. The methane partial pressures at 10 kPa are lower than those at 100 kPa in the range of short residence times, but the decrease at longer residence times is weaker (Fig. 7a). Decomposition of methane is reflected in the

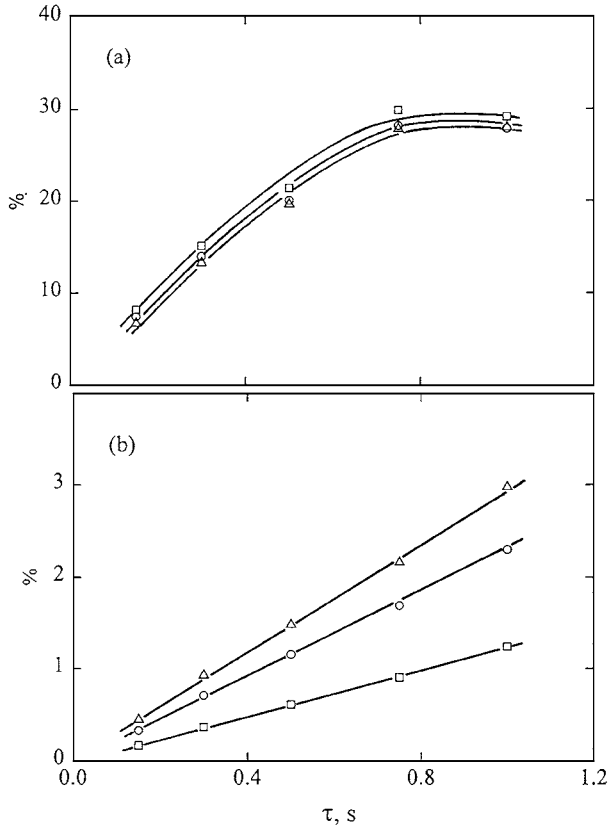

Figure 8 The fraction of carbon stored in condensing products (a), and the fraction of deposited carbon (b) related to the fed carbon. Symbols see Fig. 5.

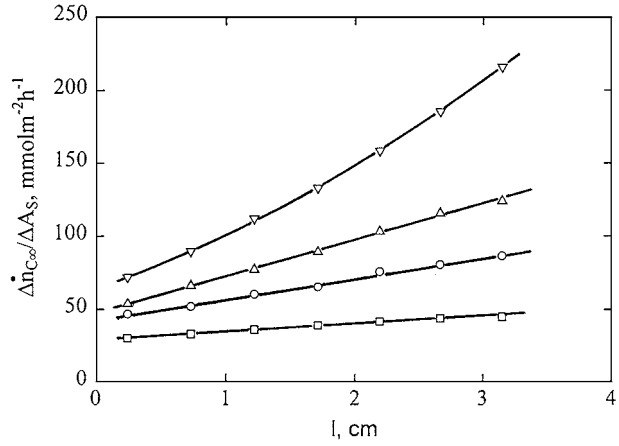

Figure 9 Steady-state surface related deposition rates as a function of substrate length at a temperature of 1100 °C, various methane pressures and a $[A_S/V_R]$ ratio of 1.65 mm^{-1},; the residence time is 1.1 s. (□) 5 kPa, (○) 10 kPa, (△) 15 kPa and (▽) 20 kPa.

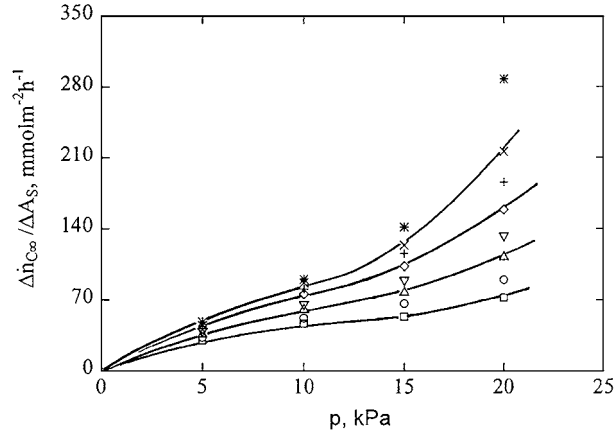

Figure 10 Steady-state surface related deposition rates at various lengths of the substrate as a function of methane pressure (results from Fig. 9); the lengths are (□) 0.485 mm, (○) 0.975 mm, (△) 1.46 mm, (▽) 1.96 mm, (◇) 2.43 mm, (+) 2.91 mm, (×) 3.40 mm and (*) 3.88 mm.

hydrogen partial pressures; they show a continuous increase at 10 kPa and an incubation at 100 kPa (Fig.7 b). Much more hydrogen is detected at 100 kPa as compared to 10 kPa at longer residence times which cannot be explained by the difference in methane decomposition. The partial pressures of both gases do not show an influence of the substrate.

The partial pressures of ethene and ethine are presented in Fig. 7c and d. The partial pressures of ethine, which is a consecutive product of ethene, show a slight incubation phase at both pressures. But it is even more remarkable that the partial pressures of both C_2-hydrocarbons at 10 kPa are much lower than those at 100 kPa. A clear influence of the substrate on the partial pressures does not exist. Condensing products were not determined. The fraction of carbon stored in these products was calculated from a carbon balance. Fig. 8a shows this fraction; it is compared with the fraction of deposited carbon (Fig. 8b). Considering the results of Fig. 7a–d indicates that the condensing products are the major products and carbon deposition is a relatively unimportant side reaction.

3.2. Various methane pressures

The above results have demonstrated that the usefulness of CVD kinetics, determined with argon and possible other gases as diluent gas, is limited for a treatment of CVI with pure methane at low pressures. Therefore, carbon deposition from pure methane was studied. Results at a $[A_S/V_R]$ ratio of 1.65 mm^{-1}, a residence time of 1.1 s and methane pressures ranging from 5 to 20 kPa are presented in Fig. 9. An increase of methane pressure leads to increasing initial rates at the beginning of the substrate and a stronger rate increase along the substrate. Thus, the rate ratios at the end of the substrate are higher than those at the beginning.

An analysis of this effect is attempted by a plot of the rates as a function of methane pressure (Fig. 10). At the beginning of the substrate (lowest curve) a hyperbolic increase of the rate suggests Langmuir-Hinshelwood kinetics, at least up to a pressure of about 15 kPa. Above this pressure the rate further increases. Similar, but less pronounced dependencies result for the upper parts of the substrate. Langmuir-Hinshelwood kinetics indicate a saturation adsorption of a major carbon forming species. Further rate increases above the pressure at which saturation adsorption is achieved may be caused by formation of larger major carbon forming species in the gas phase (aromatic or polyaromatic species) which lead to higher deposition rates.

3.3. Velocity and gas temperature profiles

The velocity profiles at room temperature and an ambient pressure of 100 kPa were experimentally

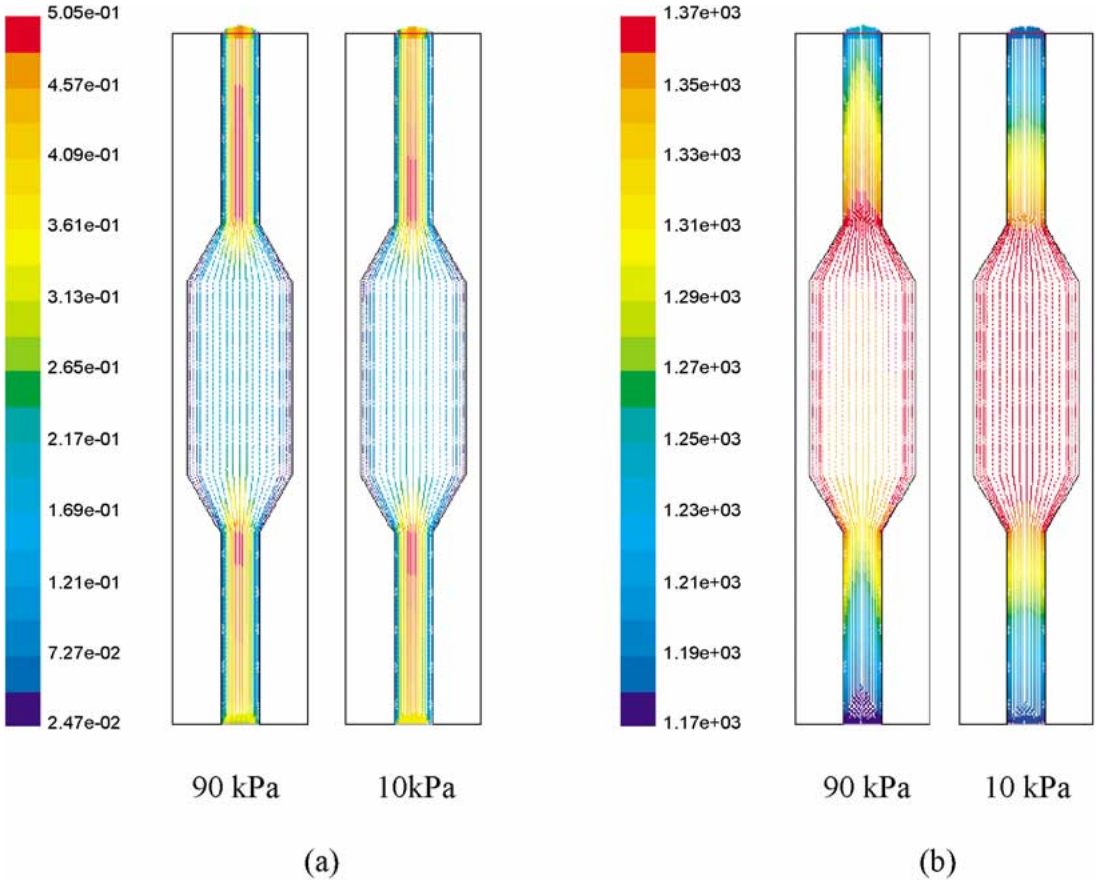

Figure 11 Simulation of the velocity distribution (a) and the temperature distribution (b) in the empty reactor tube at 90 kPa (80 kPa argon and 10 kPa methane) and 10 kPa methane; the surface temperature of the tube is 1100 °C, the residence time 1 s.

determined in an earlier study using an acrylic glass model of the reactor and ammonium chloride smoke [4]. In this study a plug flow behavior and a strong decrease of the velocity in a narrow range at the surface have been observed. The residence time distribution at 1100 °C and various residence times were determined by injecting a pulse of 1 ml methane into flowing argon. Bodenstein numbers calculated from the response signal of methane were higher than 50 which indicates a plug flow behavior under reaction conditions.

Simulation of velocity profiles in the empty reactor tube (without a substrate) was performed for a temperature of 1100 °C, pressures of 10 kPa (pure methane) and 90 kPa (80 kPa argon and 10 kPa methane) and a residence time of 1s (corresponding to a reactor length of 40 mm) using a 2 dimensional flow model. The results are presented in Fig. 11a. The velocity vectors show a small, but continuous decrease from the center to the surface. This profile corresponds neither a plug nor a parabolic flow. The influence of pressure is small.

Simulations of the temperature profiles for the same conditions are presented in Fig. 11b. They show a significant influence of pressure. At 10 kPa the temperature distribution seems to be homogeneous, whereas significant radial as well as axial temperature gradients can be observed at 90 kPa.

4. Discussion

Basis of the deposition process are chemistry and kinetics of gas phase and surface reactions. The most significant steps are summarized in the following model (Equation 2) [9, 12]:

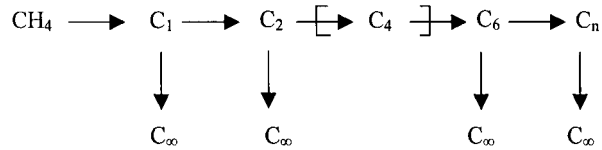

(2)

where C_1=CH_3; C_2=$C_2H_6 \cdots\cdots C_2H_2$; C_4=$C_4H_6 \cdots\cdots C_4H_4$; C_6=monocyclic aromatic hydrocarbons; C_n=polycyclic aromatic hydrocarbons; C_∞ = carbon.

The methyl radical is a decisive intermediate in the formation of larger species, but it should be unimportant for carbon deposition. Several authors postulate an autocatalysis in methane pyrolysis which implies that decomposition of methane is accelerated by radicals formed in consecutive reactions [14, 15]. Back-diffusion or back mixing, of particular importance at low pressure, may thus accelerate methane dissociation, additionally. Formation of cyclic hydrocarbons is assumed to occur via C_2 and C_4 species, although it was shown in some recent studies that C_3 species and especially the propargyl radical may be of similar importance [16].

In order to simplify the following discussion, Equation 2 is reduced to two major steps of gas phase reactions, namely formation of larger, linear hydrocarbon species and aromatic or polyaromatic hydrocarbon species (Equation 3):

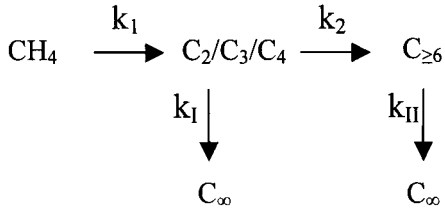

(3)

$C_{\geq 6}$ = aromatic and polyaromatic hydrocarbon species; k_1, k_2 = rate constants of gas phase reactions, s^{-1}; k_I, k_{II} = rate constants of surface reactions, s^{-1}.

This scheme is sufficient to understand increasing carbon deposition rates as the gas flows along the substrate (Figs. 2–6) because the deposition rates, r_i, increase as follows (Equation 4) [4–6]:

$$r_{C1} \ll [r_{C2} < r_{C3} < r_{C4}] \ll [r_{C6} < r_{Cn}] \qquad (4)$$

The rate increase as a function of substrate length or residence time (see Equation 1), existing at all pressures, confirms numerous earlier studies performed at 100 kPa and thus the above model. Nevertheless, pressure has a significant influence on the initial rates at the beginning of the substrate as well as on the slope of the rates as a function of substrate length. Initial rates increasing with decreasing pressure can easily be attributed to increasing temperatures, as shown in Fig. 11b. Higher initial temperatures are reflected by an advanced decomposition of methane as shown in Fig. 7a. Lower slopes at decreasing pressure and especially at 10 kPa and the longer residence time of 1.1 s are caused by the following: (1) Decreasing axial temperature gradients. (2) An increasing expansion of the gas by decomposition of methane which leads to decreasing residence times and thus a reduced formation of larger hydrocarbon species. The expansion of the gas may be derived from the lower methane partial pressures at extended residence times at 10 kPa as compared to 100 kPa (Fig. 7a). This interpretation implies that methane decomposition in the range from 10 to 100 kPa is not strongly influenced by pressure or collision with argon molecules. (3) A depletion of reactive species in the gas phase by higher deposition rates in the front part of the substrate. The latter effect is underlined by the results at a methane pressure of 20 kPa (Fig. 4) as compared to those at 10 kPa (Fig. 3b). All mentioned effects on the deposition profiles should be rather strong. Therefore, it is difficult to analyze any additional effect of diffusion as depending on pressure.

The results on the influence of $[A_S/V_R]$ ratio obtained at 90 kPa confirm those of earlier studies (Fig. 5). The results at 10 kPa (Fig. 6a and b) demonstrate that this effect also exists in depositions at low pressure. It is remarkable that the difference in deposition rate generally develops as the gas flows along the substrate. It is important to note that this is not caused by a depletion of the gas phase. The partial pressures of all detected gases do not show a pronounced influence of $[A_S/V_R]$ ratio (Fig. 7a–d). Additionally, Fig. 8b shows that the deposited fraction of the fed carbon is very low with all substrates, especially if compared with the carbon stored in the condensing products (Fig. 8a). These latter fractions indicate a small influence of $[A_S/V_R]$ ratio; it implies that the relative differences do not support the assumption of a depletion. Thus, deposition rates depending on $[A_S/V_R]$ ratio have to be attributed to different deposition chemistries or major carbon forming species. Based on Equation 3 the reaction sequences at a very low and a very high $[A_S/V_R]$ ratio could be as follows (Equations 3a and b):

$$CH_4 \longrightarrow C_2/C_3/C_4 \longrightarrow C_{\geq 6} \longrightarrow C_\infty \qquad (3a)$$

$$CH_4 \longrightarrow C_2/C_3/C_4 \longrightarrow C_\infty \qquad (3b)$$

For this reason surface related deposition rates may never be constant, but decrease with increasing surface area A_S at a constant volume V_R or increasing $[A_S/V_R]$ ratio, as mentioned in Section 1.

This property of a complex deposition process is of special importance for chemical vapor infiltration because the internal pore surface area / pore volume ratio continuously increases with progressive infiltration of a porous structure [11].

The results on the deposition rates as a function of methane pressure (Fig. 10) suggest Langmuir-Hinshelwood kinetics of the surface reactions, superimposed by gas phase reactions leading to larger species. Considering results obtained by increasing methane partial pressure at a constant total pressure of 100 kPa [6] let assume that a first step of saturation adsorption at about 15 kPa (Fig. 10) is followed by a second step at a pressure above 50 kPa.

These interpretations are supported by the experimental results which show that saturation adsorption at about 15 kPa is only pronounced at the beginning of the substrate where the formation of larger consecutive products is still limited. At the end of the substrate such consecutive products are formed in gas phase reactions, which can be recognized from a more or less continuous transition from step one to step two of saturation adsorption.

Equation 3 should represent an appropriate model for simulation of the deposition rates as a function of both methane pressure as well as the length of the substrate. The differential equations are given by Equations 4–7.

$$\frac{d[CH_4]}{d\tau_R} = -k_1[CH_4] \qquad (4)$$

$$\frac{d[C_1]}{d\tau_R} = +k_1[CH_4] - k_2[C_1] - r_{S,l}([C_1]) \qquad (5)$$

$$\frac{d[C_c]}{d\tau_R} = +k_2[C_2] - r_{S,c}([C_c]) \qquad (6)$$

$$\frac{d[C_\infty]}{d\tau_R} = +r_{S,l}([C_1]) + r_{S,c}([C_c]) \qquad (7)$$

where $[C_l]$, $[C_c]$ = concentration of linear (C_2, C_3, C_4) and cyclic species ($C_{\geq 6}$).

The surface rates r_S (Equations 11 and 12) result from the following reactions 8–10:

$$C_\infty(\,) + C_l \xrightarrow{k_I} C_\infty(H) + H_2 \tag{8}$$

$$C_\infty(\,) + C_c \xrightarrow{k_{II}} C_\infty(H) + H_2 \tag{9}$$

$$C_\infty(H) \underset{k_{ads}}{\overset{k_{des}}{\rightleftharpoons}} C_\infty(\,) + H_2 \tag{10}$$

$$r_{S,l} = \frac{c \cdot k_I[C_l]}{1 + \dfrac{k_{ads}}{k_{des}}[H_2] + \dfrac{k_I[C_l] + k_{II}[C_c]}{k_{des}}} \tag{11}$$

$$r_{S,c} = \frac{c \cdot k_{II}[C_c]}{1 + \dfrac{k_{ads}}{k_{des}}[H_2] + \dfrac{k_I[C_l] + k_{II}[C_c]}{k_{des}}} \tag{12}$$

$C_\infty(\,)$ = free active site; $C_\infty(H)$ = active site blocked with hydrogen (carbon hydrogen surface complex); c = concentration of active sites.

Introducing Equations 11 and 12 into Equations 5 and 6, respectively, the differential Equations 4 to 7 can be solved, provided appropriate boundary conditions are available and the rate constants are known, which is not the case. Initial deposition rates greater than zero (Fig. 7, $1 \rightarrow 0$) indicate a pyrolysis of methane in the preheating zone or a back-diffusion as discussed above. Back-diffusion or back mixing are difficult to include in Equations 4 to 7 because of the high number of unknown species.

It could be a first approach to demonstrate the relevance of the proposed deposition kinetics by simulation of the results of Fig.8 using Equation 7a and fitting the rate constants as well as the concentrations of C_l, C_c and H_2. The relevance of Equation 7a could be shown if two conditions are fulfilled: (1) A satisfying fit of the experimental results. (2) Reasonable concentrations of C_l, C_c and H_2.

$$\frac{d[C_\infty]}{d\tau_R} = \frac{c \cdot (k_I[C_l] + k_{II}[C_c])}{1 + \dfrac{k_{ads}}{k_{des}}[H_2] + \dfrac{k_I[C_l] + k_{II}[C_c]}{k_{des}}} \tag{7(a)}$$

The simulation will be presented in a forthcoming paper.

Acknowledgements

This research was performed in the Collaborative Research Center (Sonderforschungsbereich) 551. Financial support by the Deutsche Forschungsgemeinschaft is gratefully acknowledged.

References

1. W. BENZINGER, A. BECKER and K. J. HÜTTINGER, *Carbon* **34** (1996) 957.
2. W. V. KOTLENSKI, in "Chemistry and Physics of Carbon," edited by P. L. Walker Jr and P. A. Thrower, Vol. 9 (M. Dekker, Inc. New York, 1973), p. 173.
3. W. BENZINGER and K. J. HÜTTINGER, *Carbon* **34** (1996) 1465.
4. A. BECKER and K.J. HÜTTINGER, *ibid.* **36** (1998) 177.
5. *Idem.*, *ibid.* **36** (1998) 201.
6. *Idem.*, *ibid.* **36** (1998) 213.
7. K. J. HÜTTINGER, *Adv. Mater. CVD* **4** (1998) 151.
8. A. BECKER, Z. HU and K. J. HÜTTINGER, *Fuel* **79** (2000) 673.
9. M. TEUBNER, Z. HU and K. J. HÜTTINGER, *High Temp. - High Press.* **32** (2000) 725.
10. J. ANTES, Z. J. HU, W. G. ZHANG and K. J. HÜTTINGER, *Carbon* **37** (1999) 2031.
11. W. BENZINGER and K. J. HÜTTINGER, *ibid.* **37** (1999) 1311.
12. Z. HU and K. J. HÜTTINGER, *Adv. Mater. CVD* **6** (2000) 77.
13. Fluent Inc., FLUENT manual **5** (1999).
14. J. M. ROSCOE and M. J. THOMSON, *Int. J. of Chem. Kin. Ser.* **63** (1985) 967.
15. A. M. DEAN, *J. Phys. Chem.* **94** (1990) 1432.
16. N. M. MARINOV, W. J. PITZ, C. K. WESTBROOK, M. J. CASTALDI and S. N. SENKAN, *Combust. Sci. and Techn.* **116/117** (1996) 221.

Received 18 April
and accepted 10 October 2000